Journal of Molecular Structure 937 (2009) 10–15

Contents lists available at ScienceDirect

Journal of Molecular Structure

journal homepage: www.elsevier.com/locate/molstruc

The structure of two pyrazole esters related to Rimonabant

Ibon Alkorta [a,*], Pilar Goya [a], Ruth Pérez-Fernández [a], Mario Alvarado [a], José Elguero [a], Santiago García-Granda [b,*], Laura Menéndez-Taboada [b]

[a] Instituto de Química Médica, CSIC, Juan de la Cierva, 3, E-28006 Madrid, Spain
[b] Departamento de Química Física y Analítica, Facultad de Química, Universidad de Oviedo, E-33006 Oviedo, Spain

ARTICLE INFO

Article history:
Received 13 July 2009
Received in revised form 30 July 2009
Accepted 3 August 2009
Available online 25 August 2009

Keywords:
Rimonabant
Pyrazole
X-ray
NMR
B3LYP
GIAO

ABSTRACT

Two 1,5-diarylpyrazoles related to the antiobesity agent Rimonabant have been synthesized and their structure determined by X-ray crystallography. Compound **2**, 1-(2,4-dichlorophenyl)-5-(4-chlorophenyl)-4-methyl-1*H*-pyrazole-3-carboxylate, forms strange crystals but its only peculiarity involves Cl···Cl and Cl···π interactions, that were modeled theoretically at the M05-2x/6-31+G(d,p) level. ^{13}C NMR results were rationalized through GIAO calculations at the B3LYP/6-311+G(d,p) computational level.

1. Introduction

Rimonabant [1,2], the first CB1 antagonist approved in the EU for the treatment of obesity had to be withdrawn from the market due to psychiatric side effects. The development of other related structures (Scheme 1) has also been discontinued for similar reasons. However, we and others are still working on these structures trying to suppress the unwanted central side-effects [3–6] of CB1 antagonists and to discover new CNS properties. We have already published a paper describing a pyrazole fatty acid amide family designed as multiple ligands with antiobesity and hypophagic properties [7].

We present here the structural study of two esters, **1** and **2** (Scheme 2) used as precursors of some biologically active compounds.

2. Results and discussion

2.1. Solid-state structures

We have recently published the structural studies of Rimonabant [8] and compounds **3–5** [9]. The Rimonabant studies included X-ray crystallography and NMR data. First, the X-ray molecular structures of compounds **1** and **2** will be described. Compound **1** crystals were colorless but those of **2** formed some hemispherical shaped aggregates of orange crystals (Fig. 1) resembling an orange fruit.

The molecular structure of compound **1** is shown in Figs. 2 and 3 while Figs. 4 and 5 are for compound **2**. The single crystal X-ray data for both structures are listed in Table 3. Hydrogen-bonding geometry for compound **1** is collected in Table 4 (see Section 3). The crystal packing of compound **1** at 100 K shows a helix along *a* axis as shown in Fig. 6. The helical structure is sustained by hydrogen bonds involving oxygen and carbon (C15—H15···O2), forming an infinite chain. No conventional hydrogen bonds were found at RT for **1**, neither for compound **2**.

The aryl rings of compounds **1** and **2** (Table 1) were neither planar nor perpendicular being close to 45 °C. The change in temperature in compound **1** affects significantly the torsion angles, becoming both angles alike at 100 K. The calculated geometry (monomer in the gas phase) had lower values but it resembled the 293 K structure. In compound **2**, the presence of an *ortho* chlorine atom increased 10° the dihedral angle of the *N*-aryl group. The calculated geometry of the monomer exaggerated this angle. In the dimer model (which has an H atom in the place of the ester group) the angles were modified but further removed from the experimental values.

Compound **2** crystallized forming dimers stabilized by halogen bonds between the *C*-*p*-chlorophenyl and the *N*-*o*-chlorophenyl (Cl···Cl = 3.46 Å) and by Cl···π interactions between the *C*-*p*-chlorophenyl and the opposite *p*-chlorophenyl (Cl···centroid = 4.01 Å,

* Corresponding authors. Tel.: +34 91 5622900; fax: +34 91 5644853 (I. Alkorta).
E-mail address: ibon@iqm.csic.es (I. Alkorta).

0022-2860/$ - see front matter © 2009 Elsevier B.V. All rights reserved.
doi:10.1016/j.molstruc.2009.08.018

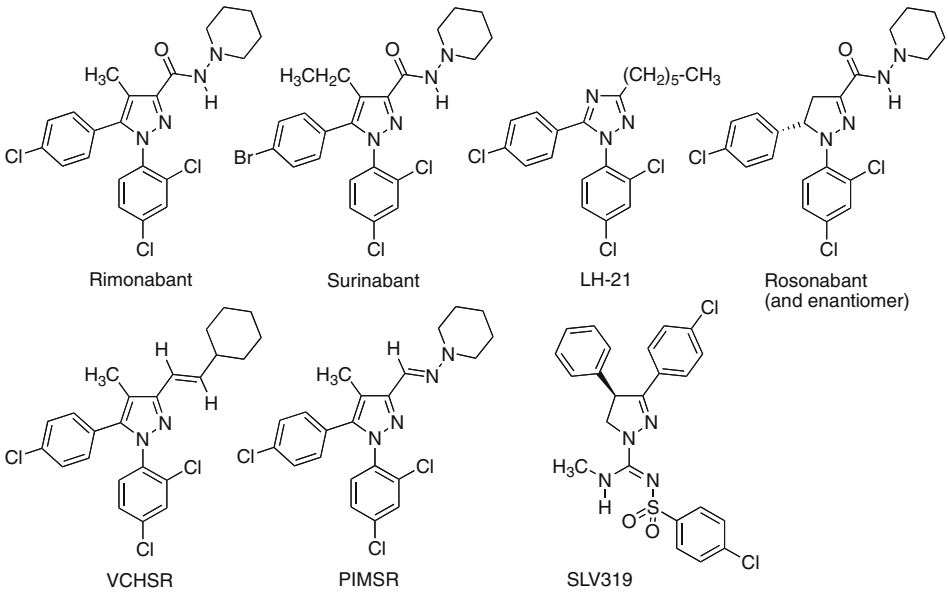

Scheme 1.

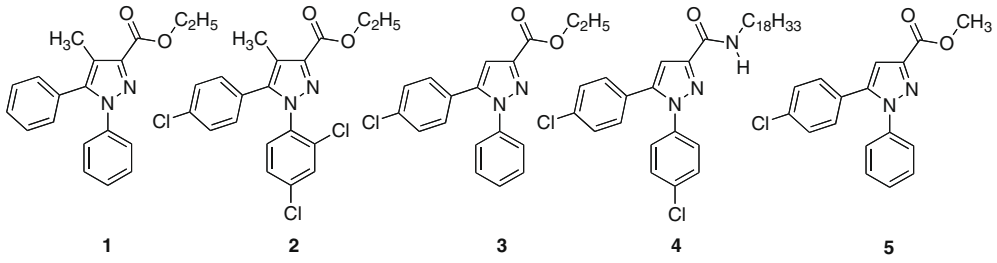

Scheme 2.

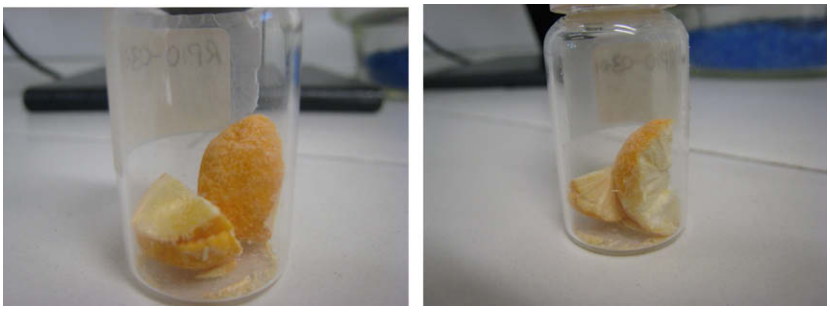

Fig. 1. Compound **2** crystals (vial diameter 2 cm).

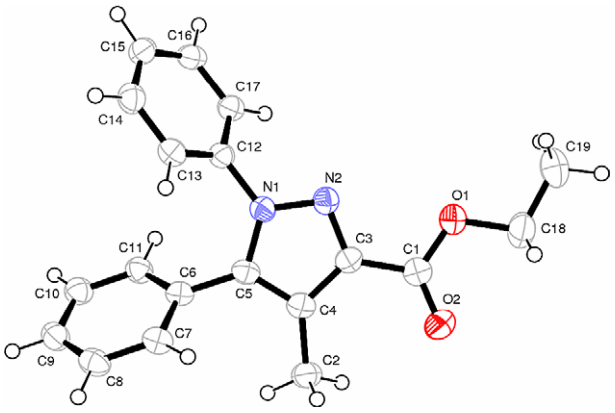

Fig. 2. An ORTEP view of an isolated molecule of compound **1**.

Cl···closet C = 3.96 Å) (Fig. 1). Compound **5** (GOKFUI) [10] did not present any similar interaction but compound **4** (GOKGAP) [10] showed a Cl···centroid distance of 3.62 Å and Cl···closet C distance of 3.43 Å between the Cl of the 5-aryl group and the aryl of the 1-phenyl group [9].

In order to study the molecular interactions observed within the X-ray structure, a model of the dimer $\mathbf{2}_2$ was optimized with the M05-2x/6-31+G* computational level (see Section 3.2.2), a functional known to yield good stacking energies. The structure was very similar (see Fig. 8) to Fig. 7. This model corresponded to the replacement of the ethoxycarbonyl groups by H atoms (compound $\mathbf{2a}_2$). Calculations of the frequencies have been carried out to confirm that the structure obtained correspond to energetic minima. The electron density has been analyzed within the atoms in molecules (AIM) methodology with the AIM2000 program. The calculated interaction energy accounts to -16.7 kJ mol^{-1}.

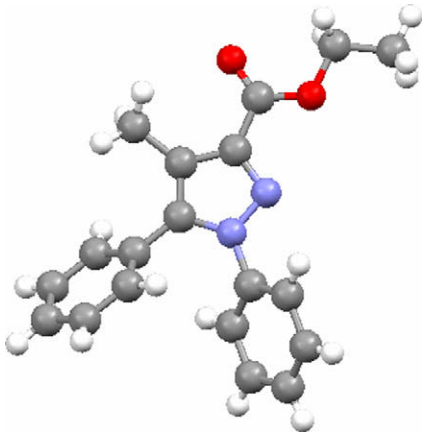

Fig. 3. X-ray molecular structure of compound **1** (100 K).

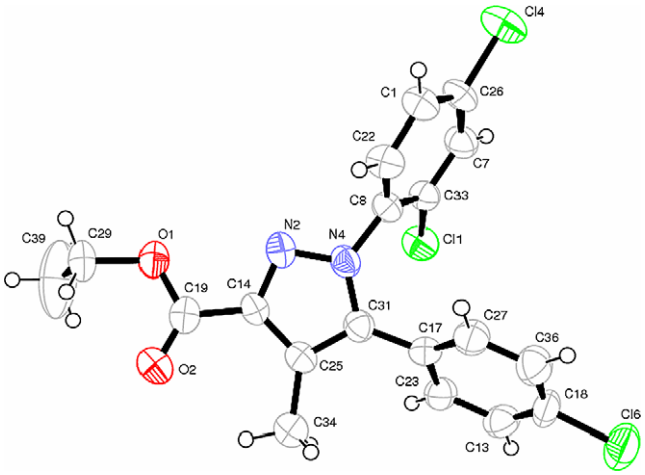

Fig. 4. An ORTEP view of an isolated molecule of compound **2**.

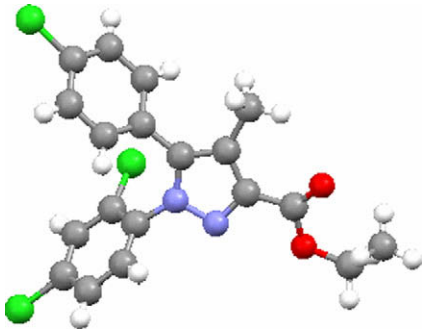

Fig. 5. X-ray molecular structure of compound **2**.

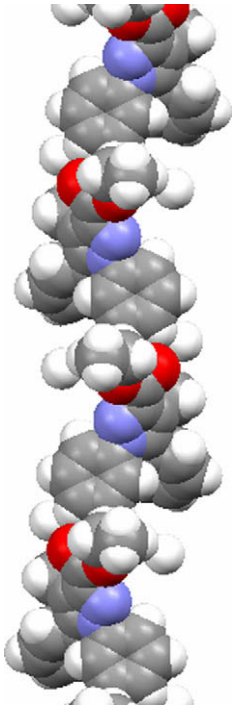

Fig. 6. Helical structure of compound **1** (100 K).

Table 1
Torsion angles (°) of the phenyl rings of compounds **1** and **2**.

Compd.	Temp. (K)	N—Ar	C—Ar	Calc.	N—Ar	C—Ar
1	293	49.0	57.6	Monomer	43.2	54.2
	100	51.0	53.4			
2	293	59.1	52.9	Monomer	65.5	50.8
				Dimer	67.2	45.0

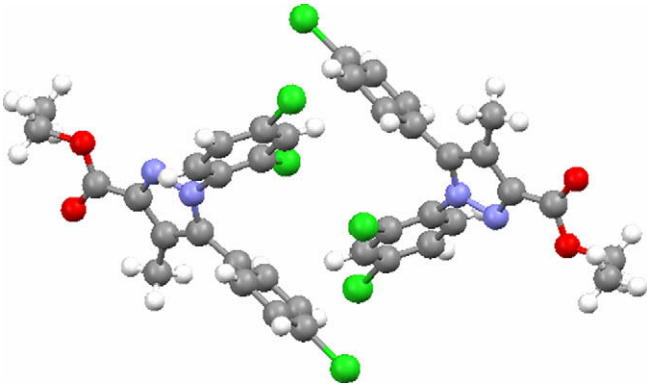

Fig. 7. View of the dimer of compound **2**.

An AIM analysis yielded the following picture (Fig. 8). Four intermolecular bond critical points (bcp) are found, two of them corresponding to Cl···Cl interaction and another two to Cl···aromatic carbon interactions. In the first case, the distance between the halogen atoms is of 3.52 Å and they are in a perpendicular orientation, orientation that have been shown to be the most favorable disposition in order to minimize their electronic repulsion [11,12]. The values of the electron density and Laplacian for this bcp (0.006 and 0.023 au, respectively) indicate that it corresponds to a closed shell interaction. The second set of bcp's accounts for the interaction of one chlorine atom and one of the aromatic carbon atoms that are located at a distance of 3.63 Å. As previously, the electron density and Laplacian values of these bcp's (0.005 and 0.015 au, respectively) are indicative of closed shell interactions similar to those find in weak contacts with the π-cloud of aromatic systems [13,14].

2.2. NMR results and GIAO calculations

We have gathered in Table 2 the experimental and calculated ^{13}C chemical shifts (δ ppm) of compounds **1** and **2** together with

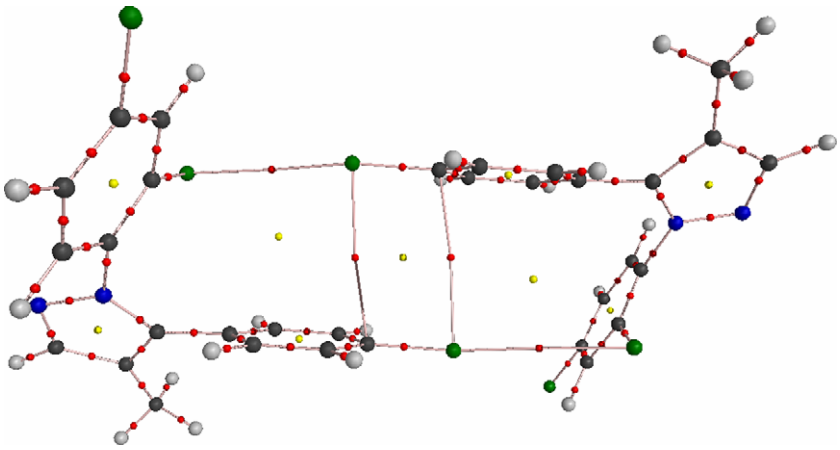

Fig. 8. View of the molecular graph of the dimer of model compound **2a**. The position of the bond and ring critical points are indicated with red and yellow points. The bond paths are shown. (For interpretation of the references to color in this figure legend, the reader is referred to the web version of this paper.)

Table 2
^{13}C NMR absolute shieldings and chemical shifts of compounds **1** and **2** (all values in ppm).

Compd.	Atom	σ	δ calcd.	δ exp.
1	C3	34.6488	142.33	145.0
	C4	52.4872	125.15	119.0
	C5	35.0231	141.97	141.1
	C1′	35.0390	141.96	141.0
	C2′/C6′	52.1178	125.51	124.3
	C3′/C5′	49.6484	127.89	127.9
	C4′	51.4920	126.11	126.7
	C1″	44.6039	132.75	132.5
	C2″/C6″	45.9203	131.48	129.0
	C3″/C5″	49.5063	128.03	128.5
	C4″	49.8313	127.71	127.5
	4-Me	171.6946	10.36	8.4
	C=O	13.3933	162.80	162.2
	CH_2	118.4583	61.62	61.1
	CH_3	168.1801	13.74	14.3
2	C3	33.7715	143.18	143.0
	C4	54.3330	123.38	119.2
	C5	33.1665	143.76	142.9
	C1′	38.4531	138.67	136.1
	C2′	35.7526	141.27	133.1[a]
	C3′	47.7768	129.69	130.1
	C4′	32.6966	144.21	136.0[a]
	C5′	50.8738	126.71	127.8
	C6′	45.4809	131.90	130.7
	C1″	48.0830	129.40	127.1
	C2″/C6″	45.9051	131.49	130.9
	C3″/C5″	49.1703	128.35	128.9
	C4″	32.8185	144.10	135.0[a]
	4-Me	171.0935	10.94	9.7
	C=O	13.7655	162.44	162.8
	CH_2	119.5178	60.60	61.0
	CH_3	167.6242	14.28	14.4

[a] C—Cl atoms.

the absolute shieldings (σ ppm) calculated at the GIAO/B3LYP/6-311++G(d,p)//B3LYP/6-311++G(d,p) level (see Section 3.2.2). To transform σ into δ we used an equation established empirically from a set of 461 points [15]: $\delta^{13}C = 175.7 - 0.963\ \sigma^{13}C$. The experimental values have been assigned by traditional 2D experiments including NOESY [16].

As we have previously reported, carbon atoms bearing chlorine substituents such as C2′, C4′ and C4″ deviated systematically from the calculated values around −7.7 ppm (previously we have found −8.7 ppm [8] and −8.2 ppm [9]). The remaining points are fitted to $\delta^{13}C$ exp. = (0.994 ± 0.003) $\delta^{13}C$ calcd., $n = 29$, $R^2 = 1.000$ (black line in Fig. 9).

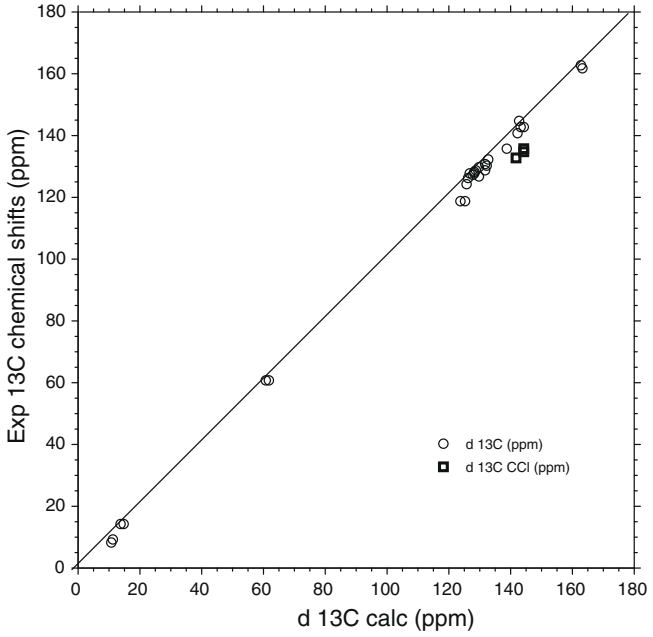

Fig. 9. Scatter of ^{13}C NMR results.

The excellence of the correlation makes unnecessary the use of additivity schemes so popular in the past. However, we have checked comparing **1** and **2** that the signals of the phenyl rings are consistent with the chlorine substituent effects [17].

3. Experimental

All chemicals were purchased from commercial suppliers and used without further purification. TLC: precoated silica-gel *60* F_{254} plates (Merck), detection by UV light (254 nm). Flash-column Chromatography (FC): *Kieselgel 60* (230–400 mesh; *Merck*). Melting points (mp) were determined in open capillaries with a *Gallenkamp* capillary melting-points apparatus and are uncorrected. ^{1}H and ^{13}C NMR spectra were recorded on Bruker Advance 300 spectrometer operating at 300.13 MHz and 75.47 MHz respectively, in $CDCl_3$ as solvent and Me_4Si as the internal standard. Chemical shifts are reported in ppm on the δ scale. The mass spectra (EI-MS; 70 eV) were determined on a MSD 5973 Hewlett Packard instrument. Since compounds **1** [18] and **2** [19] were only reported in patents we will describe them here.

3.1. Synthesis of ethyl 1,5-diphenyl-4-methyl-1H-pyrazole-3-carboxylate **1**

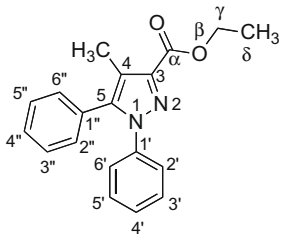

1

To a solution of ethyl 3-methyl-4-phenyl-2,4-dioxobutanoate [20] (1.60 g, 6.83 mmol) in a mixture 1:1 of EtOH/H_2SO_4 (20 mL) was added phenylhydrazine (0.73 g, 6.83 mmol). The reaction mixture was refluxed for 12 h and later evaporated under reduced pressure to give a residue which was treated with aqueous 1 N NaOH and extracted with CH_2Cl_2. The extract was dried (Na_2SO_4) and the solvent was evaporated off to give predominantly 1*H*-pyrazole-3-carboxylate isomer as a viscous yellow oil. The product was purified by FC (SiO_2; EtOAc/*n*-hexane 1:3) and crystallization (0.5 g, 24% yield). Yellowish solid, mp: 105–106 °C (EtOH); MS/EI: *m/z* (%) = 306 (100), 234 (24); ^{1}H NMR (300 MHz, $CDCl_3$): δ = 7.30–7.05 (m, 10H), 4.38 (q, *J* = 7.0 Hz, 2H), 2.37 (s, 3H), 1.34 (t, *J* = 7.0 Hz, 3H); ^{13}C NMR (75 MHz, $CDCl_3$): δ = 162.2 (Cα), 145.0 (C3), 141.1 (C5), 141.0 (C1′), 132.5 (C1″), 129.0 (C2″ & C6″), 128.5 (C3″ & C5″), 127.9 (C3′ & C5′), 127.5 (C4″), 126.7 (C4′), 124.3 (C2′ & C6′), 119.0 (C4), 61.1 (Cγ), 14.3 (Cδ), 8.4 (C—CH_3). Elemental analysis calc. for $C_{19}H_{18}N_2O_2$ (306.36) C: 74.49; H: 5.92; N: 9.14. Found: C: 74.28; H: 6.01; N: 9.24.

3.2. Synthesis of ethyl 1-(2,4-dichlorophenyl)-5-(4-chlorophenyl)-4-methyl-1H-pyrazole-3-carboxylate **2**

A mixture of **6** (5.56 g, 0.02 mmol) and 2,4-dichlorophenylhydrazine (4.3 g, 0.02 mmol) was dissolved in EtOH (150 mL). Then, H_2SO_4, 50% (60 mL) was carefully added. The reaction mixture was heated at 100 °C for 16 h. The mixture was cooled down to room temperature and poured into an ice bath. The precipitated was filtered and the solid washed extensively with water. Then, the brownish sticky solid was dissolved in Et_2O (30 mL) and washed with water (2 × 30 mL). The organic layers were evaporated under reduced pressure and the crude purified by column chromatography (eluent: DCM + 0.1% MeOH) yielding a light yellow solid (4.27 g, 52%). M.p. 126–128 °C. ^{1}H NMR (300 MHz, $CDCl_3$) δ 7.40 − 7.13 (m, 5H, C3′, C5′, C6′, C3″), 7.02–6.99 (m, 2H, C2″), 4.38 (q, *J* = 7.1 Hz, 2H, Cγ), 2.26 (s, 3H, C—CH_3), 1.36 (t, *J* = 7.1 Hz, 3H, Cδ). ^{13}C NMR (75 MHz, $CDCl_3$) δ 162.8 (Cα), 143.0 (C3), 142.9 (C5), 136.1 (C1′), 136.0 (C4′), 135.0 (C4″), 133.1 (C2′), 130.9 (C2″ & C6″), 130.7 (C6′), 130.1 (C3′), 128.9 (C3″ & C5″), 127.8 (C5′), 127.1 (C1″), 119.2 (C4), 61.0 (Cγ), 14.4 (Cδ), 9.7 (C—CH_3). Elemental analysis calc. for $C_{19}H_{15}Cl_3N_2O_2$ (409.69) C: 55.70; H: 3.69; N: 6.84. Found: C: 55.59; H: 3.81; N: 6.94. HPLC–MS: A: Acetonitrile + 0.01% formic acid, B: Water + 0.01% formic acid. Grad from 10% to 100% of A in 5 min, 100% of A for 2 min; column SunFire C18 3.5 μm. 4.6 × 50 mm. Flow 1 mL/min. *m/z* 411.3, t = 6.19 min.

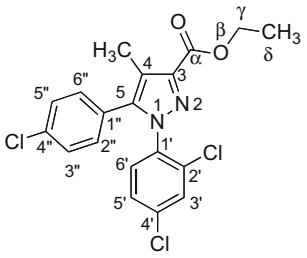

2

3.2.1. Crystallography

Colorless crystals from compound **1** and **2** were used for data collection at 100 K and RT, for **1**, and only a RT for **2**. Mirror-monochromated radiation CuK/a, λ = 1.54184 Å was used in all cases. A total of 6618 ($-14 \leqslant h \leqslant 11$, $-12 \leqslant k \leqslant 12$, $-17 \leqslant l \leqslant 16$) reflections were collected for compound **1** at 100 K with 2740 independent reflections, while 13206 ($-14 \leqslant h \leqslant 14$, $-12 \leqslant k \leqslant 12$, $-17 \leqslant l \leqslant 17$) reflections were collected for compound **1** at RT, with 2936 independent reflections. For compound **2**, 15425 ($-27 \leqslant h \leqslant 21$, $-9 \leqslant k \leqslant 7$, $-25 \leqslant l \leqslant 27$) reflections were collected, with 3688 independent reflections. Data collection for all measurements was made using the program CrysAllis CCD [21]. Crystal structure was solved by Direct Methods, using the program Sir92 [22]. Anisotropic least-squares refinement was carried out with SHELXL-97 [23]. Further details of the X-ray structural analysis are given in Tables 3 and 4. Geometrical calculations were made

Table 3
Crystal data and structure refinement for compounds **1** and **2**.

Compound	**1**	**1**	**2**
Empirical formula	$C_{19}H_{18}N_2O_2$	$C_{19}H_{18}N_2O_2$	$C_{19}H_{15}Cl_3N_2O_2$
Formula weight	306.35	306.35	409.68
Temperature (K)	100(2)	293(2)	293(2)
Wavelength (Å)	1.54184	1.54184	1.54184
Crystal system	Monoclinic	Monoclinic	Orthorhombic
Space group	$P2_1/c$	$P2_1/c$	Pbca
α (Å)	12.4168(3)	12.3959(10)	22.042(3)
β (Å)	10.6745(2)	10.5622(5)	7.7499(16)
χ (Å)	14.5062(6)	14.957(2)	22.375(3)
a (°)	90	90	90
b (°)	121.994(2)	119.816(8)	90
g (°)	90	90	90
V (Å^3)	1630.65(8)	1699.1(3)	3822.2(11)
Z	4	4	8
m (mm^{-1})	0.656	0.630	4.477
F(0 0 0)	648	648	1680
Crystal size (mm)	0.26 × 0.21 × 0.08	0.26 × 0.19 × 0.15	0.14 × 0.05 × 0.014
Reflections collected	6618	13206	16759
Unique reflections	2740	2936	3688
R(int)	0.0362	0.0237	0.1613
$R_1[I > 2\sigma(I)]$	0.0380	0.0369	0.0466
wR_2 (all data)	0.0891	0.1156	0.0946

Table 4
Hydrogen bonds for compound **1** at 100 K (Å, °).

D—H···A (Å)	D—H (Å)	H···A (Å)	D···A (Å)	D···A (°)	Symmetry[a]
C15—H15···O2	0.91(2)	2.61(2)	3.346(2)	138.4(16)	1

[a] Symmetry transformations used to generate equivalent atoms: (1) $x+1$, $-y-1/2$, $z+1/2$.

with PARST97 [24] and molecular graphics with ORTEP-3 [25] for Windows.

3.2.2. Computational details

The optimization of the geometries of the structures were first carried out at the B3LYP/6-31G* (and then reoptimized at the B3LYP/6-311++G** computational level [26–31] within the Gaussian-03 package [32]. Frequency calculations at the B3LYP/6-31G* were carried out to confirm that the obtained structures correspond to energy minima. GIAO absolute shieldings [33,34] were calculated on the B3LYP/6-311++G** optimized geometries [B3LYP/6-311++G(d,p)//B3LYP/6-311++G(d,p)]. The structure of the dimer has been obtained using the M052x functional [35] and the 6-31+G(d,p) basis set. This functional has been shown to be suitable for the description of a variety of weak molecular interactions [36].

Acknowledgements

This work was carried out with financial support from the Ministerio de Educación y Ciencia (Project No. CTQ2007-62113 and 61901/BQU) and Comunidad Autónoma de Madrid (Project MADRISOLAR, ref. S-0505/PPQ/0225). Mario Alvarado acknowledges a Grant from RETICS RD06/001/0014 (Instituto de Salud Carlos III). S.G.-G. gratefully acknowledges the financial support from MEC, projects MAT2006-01997 and Consolider Ingenio-2010, 'Factoría Española de Cristalización'.

References

[1] M. Rinaldi-Carmona, F. Barth, M. Héaulme, D. Shire, B. Calandra, C. Congy, S. Martinez, J. Maruani, G. Néliat, D. Caput, P. Ferrara, P. Soubrié, J.C. Brelière, G. Le Fur, FEBS Lett. 350 (1994) 240.
[2] M. Rinaldi-Carmona, F. Barth, C. Congy, S. Martinez, D. Oustric, A. Pério, M. Poncelet, J. Maruani, M. Arnone, O. Finance, P. Soubrié, G. Le Fur, J. Pharmacol. Exp. Theraput. 310 (2004) 905.
[3] (a) N. Jagerovic, L. Hernández-Folgado, I. Alkorta, P. Goya, M. Navarro, A. Serrano, F. Rodríguez de Fonseca, M.T. Dannert, A. Alsasua, M. Suardíaz, D. Pascual, M.I. Martín, J. Med. Chem. 47 (2004) 2939;
(b) F.J. Pavon, A. Bilbao, L. Hernández-Folgado, A. Cipitelli, N. Jagerovic, G. Abellán, M.I. Rodríguez-Franco, A. Serrano, M. Macias, R. Gómez, M. Navarro, P. Goya, F. Rodríguez de Fonseca, Neuropharmacology 51 (2006) 358;
(c) F.J. Pavon, A. Serrano, V. Pérez-Valero, N. Jagerovic, L. Hernández-Folgado, F.J. Bermúdez-Silva, M. Macias, P. Goya, F. Rodríguez de Fonseca, J. Neuroendocrinol. Suppl. 1 (2008) 116;
(d) L. Hernández-Folgado, P. Goya, J. Frigola. M.R. Cuberes, A. Dordal, J. Holenz, N. Jagerovic, Monatsh. Chem. 139 (2008) 1073.
[4] WHO Drug Information 21 (2007) 162.
[5] D. Hurst, U. Umejiego, D. Lynch, H. Seltzman, S. Hyatt, M. Roche, S. McAllister, D. Fleischer, A. Kapur, M. Abood, S. Shi, J. Jones, D. Lewis, P. Reggio, J. Med. Chem. 49 (2006) 5969.
[6] H. Pettersson, A. Bülow, F. Ek, J. Jensen, L.K. Ottesen, A. Fejzic, J.N. Ma, A.L. Del Tredici, E.A. Currier, L.R. Gardell, A. Tabatabaei, D. Craig, K. McFarland, T.R. Ott, F. Piu, E.S. Burstein, R. Olsson, J. Med. Chem. 52 (2009) 1975.
[7] M. Alvarado, P. Goya, M. Macías-González, F.J. Pavón, A. Serrano, N. Jagerovic, J. Elguero, A. Gutiérrez-Rodríguez, S. García-Granda, M. Suardíaz, F. Rodríguez de Fonseca, Bioorg. Med. Chem. 16 (2008) 10098.
[8] I. Alkorta, M. Alvarado, J. Elguero, S. García-Granda, P. Goya, M.L. Jimeno, L. Menéndez-Taboada, Eur. J. Med. Chem. 44 (2009) 1864.
[9] I. Alkorta, M. Alvarado, J. Elguero, S. García-Granda, P. Goya, L. Torre-Fernández, L. Menéndez-Taboada, J. Mol. Struct. 920 (2009) 82.
[10] CSD database version 5.28 (November 2006). Jan-07 and May-07 updates;
(a) F.H. Allen, Acta Crystallogr. Sect. B 58 (2002) 380;
(b) F.H. Allen, W.D.S. Motherwell, Acta Crystallogr. Sect. B 58 (2002) 407.
[11] I. Alkorta, F. Blanco, J. Elguero, Struct. Chem. 20 (2009) 63.
[12] T.T.T. Bui, S. Dahaoui, C. Lecomte, G.R. Desiraju, E. Espinosa, Angew. Chem. Int. Ed. 48 (2009) 3838.
[13] I. Alkorta, I. Rozas, J. Elguero, J. Org. Chem. 62 (1997) 4687.
[14] I. Rozas, I. Alkorta, J. Elguero, J. Phys. Chem. A 101 (1997) 9457.
[15] F. Blanco, I. Alkorta, J. Elguero, Magn. Reson. Chem. 45 (2007) 797.
[16] S. Braun, H.O. Kalinowski, S. Berger, 150 and More Basic NMR Experiments, Wiley-VCH, Weinheim, 1998.
[17] J.B. Stothers, Carbon-13 NMR Spectroscopy, Academic Press, New York, 1972.
[18] N. Kanaya, H. Ishihara, Y. Kimura, T. Ishiyama, Y. Ochiai, PCT Int. Appl. (2004). WO 2004069824 A1 20040819.
[19] F. Barth, P. Casellas, C. Congy, S. Martinez, M. Carmona, Eur. Pat. Appl. (1993). 576357 A1.
[20] V.K. Kotagiri, S. Suthrapu, J.M. Reddy, C.P. Rao, V. Bollugoddu, A. Bhattacharya, R. Bandichhor, Org. Proc. Res. Dev. 11 (2007) 910.
[21] Oxford Diffraction, 2008.
[22] A. Altomare, G. Cascarano, C. Giacovazzo, A. Gualardi, J. Appl. Cryst. 26 (1993) 343–350.
[23] G.M. Sheldrick, SHELXL-97. University of Gottingen. A computer program for refinement of crystal structures, 1997.
[24] M. Nardelli, Comput. Chem. 7 (1983) 95.
[25] L.J. Farrugia, J. Appl. Cryst. 30 (1997) 565.
[26] A.D. Becke, Phys. Rev. A 38 (1988) 3098.
[27] A.D. Becke, J. Chem. Phys. 98 (1993) 5648.
[28] C. Lee, W. Yang, R.G. Parr, Phys. Rev. B 37 (1988) 785.
[29] P.A. Hariharan, J.A. Pople, Theor. Chim. Acta 28 (1973) 213.
[30] R. Ditchfield, W.J. Hehre, J.A. Pople, J. Chem. Phys. 54 (1971) 724.
[31] M.J. Frisch, J.A. Pople, R. Krishnam, J.S. Binkley, J. Chem. Phys. 80 (1984) 3265.
[32] M.J. Frisch, G.W. Trucks, H.B. Schlegel, G.E. Scuseria, M.A. Robb, J.R. Cheeseman, J.A. Montgomery Jr., T. Vreven, K.N. Kudin, J.C. Burant, J.M. Millam, S.S. Iyengar, J. Tomasi, V. Barone, B. Mennucci, M. Cossi, G. Scalmani, N. Rega, G.A. Petersson, H. Nakatsuji, M. Hada, M. Ehara, K. Toyota, R. Fukuda, J. Hasegawa, M. Ishida, T. Nakajima, Y. Honda, O. Kitao, H. Nakai, M. Klene, X. Li, J.E. Knox, H.P. Hratchian, J.B. Cross, C. Adamo, J. Jaramillo, R. Gomperts, R.E. Stratmann, O. Yazyev, A.J. Austin, R. Cammi, C. Pomelli, J.W. Ochterski, P.Y. Ayala, K. Morokuma, G.A. Voth, P. Salvador, J.J. Dannenberg, V.G. Zakrzewski, S. Dapprich, A.D. Daniels, M.C. Strain, O. Farkas, D.K. Malick, A.D. Rabuck, K. Raghavachari, J.B. Foresman, J.V. Ortiz, Q. Cui, A.G. Baboul, S. Clifford, J. Cioslowski, B.B. Stefanov, G. Liu, A. Liashenko, P. Piskorz, I. Komaromi, R.L. Martin, D.J. Fox, T. Keith, M.A. Al-Laham, C.Y. Peng, A. Nanayakkara, M. Challacombe, P.M.W. Gill, B. Johnson, W. Chen, M.W. Wong, C. Gonzalez, J.A. Pople, Gaussian 03, Gaussian, Inc., Pittsburgh PA, 2003.
[33] R. Ditchfield, Mol. Phys. 27 (1974) 789.
[34] F. London, J. Phys. Radium 8 (1937) 397.
[35] Y. Zhao, N.E. Schultz, D.G. Truhlar, J. Chem. Theory Comput. 2 (2006) 364.
[36] (a) Y. Zhao, D.G. Truhlar, J. Phys. Chem. C 112 (2008) 6860;
(b) Y. Zhao, D.G. Truhlar, Acc. Chem. Res. 41 (2008) 157.